

## Excitation of the 2.65 MeV state in the $^{20}\text{Ne}(p,n)^{20}\text{Na}$ reaction at 135 MeV

B. D. Anderson, B. Wetmore, A. R. Baldwin, L. A. C. Garcia, D. M. Manley, R. Madey, J. W. Watson, and W. M. Zhang  
*Department of Physics and Center for Nuclear Research, Kent State University, Kent, Ohio 44242*

B. A. Brown  
*Department of Physics and Astronomy, Michigan State University, East Lansing, Michigan 48824*

C. C. Foster and Y. Wang  
*Indiana University Cyclotron Facility, Bloomington, Indiana 47405*

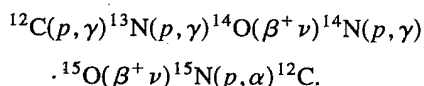
(Received 22 March 1995)

The  $^{20}\text{Ne}(p,n)^{20}\text{Na}$  reaction at 135 MeV was studied experimentally using the beam-swinger neutron time-of-flight facility at the Indiana University Cyclotron Facility. Backgrounds  $\sim 10\times$  lower than an earlier experiment were obtained using the "stripper loop" storage ring to achieve  $\sim 2\ \mu\text{s}$  between beam bursts. We were able to see a weakly excited state at 2.65 MeV in  $^{20}\text{Na}$  with a  $\Delta l=2$  angular distribution. The angular distribution is consistent with a DWIA calculation assuming a  $3^+$  final state. The characteristics of this state are important to know for considerations of possible breakout in the hot CNO cycle in supernovae explosions.

PACS number(s): 25.40.Kv, 21.60.Cs, 24.10.Eq, 27.30.+t

### I. INTRODUCTION

At the high temperatures and densities present in supernovae explosions and cataclysmic binaries, explosive hydrogen burning proceeds through the hot carbon-nitrogen-oxygen (CNO) cycle,



At very high temperatures ( $T > 3 \times 10^8$  K), the reaction sequence  $^{15}\text{O}(\alpha,\gamma)^{19}\text{Ne}(p,\gamma)^{20}\text{Na}$  may begin a sequence of rapid proton captures and beta decays that can process CNO seed nuclei to form elements up to  $A=56$  and can increase nuclear energy generation significantly [1]. This branching may also explain overabundances of Ne, Na, Mg, and Al isotopes in nova ejecta [2] and cosmic rays [3] relative to solar abundances.

The strength of this possible breakout branching is very sensitive to resonances in the  $^{19}\text{Ne} + p$  system, i.e., states in  $^{20}\text{Na}$  near the proton threshold, which is at 2.199 MeV [1]. The first state known above this threshold is one at 2.646 MeV [4]. This state was first observed via the  $^{20}\text{Ne}(^3\text{He},t)^{20}\text{Na}$  reaction [1,5-7]. Kubono *et al.* [6] identified the level as a  $1^+$  state by comparing their  $^{20}\text{Ne}(^3\text{He},t)^{20}\text{Na}$  angular distributions with distorted-wave Born approximation (DWBA) calculations. Lamm *et al.* [5,7] arrived at the same  $J^\pi$  assignment from a similar analysis. Finally, this assignment seemed to be confirmed by Clarke *et al.* [8] who made a tentative  $1^\pm$  assignment by comparing  $^{20}\text{Ne}(^3\text{He},t)^{20}\text{Na}$  and  $^{20}\text{Ne}(t,^3\text{He})^{20}\text{F}$  angular distributions for analog states.

The  $J^\pi = 1^+$  assignment was somewhat surprising because no evidence was seen for this state in an earlier  $^{20}\text{Ne}(p,n)^{20}\text{Na}$  experiment at 135 MeV [9]. The  $(p,n)$  reaction above 100 MeV is known to excite Gamow-Teller ( $\Delta l=0, \Delta s=1$ ) transitions strongly [10-12], and this transi-

tion from  $J^\pi=0^+$  to  $J^\pi=1^+$  would be such an excitation. Other  $1^+$  transitions were observed, including to the well-known  $1^+$  state at 1.00 MeV and to states at 3.0 and 3.3 MeV. The  $1^+$  assignment was questioned further in a later work of Kubono *et al.* [13] who looked at the  $\beta$ -delayed proton decay of  $^{20}\text{Mg}$  and found no evidence for any  $\beta$ -decay transition to the 2.65 MeV state. They did see  $\beta$  decay to other  $1^+$  states in  $^{20}\text{Na}$ , including the  $1^+$  states at 1.00 MeV and 3.0 MeV. Another experiment of this type was performed also by Piechaczek *et al.* [14] who observed the  $\beta$ -delayed proton decay and  $\gamma$  decay from  $^{20}\text{Mg}$  implanted into a silicon detector array at GANIL. Piechaczek *et al.* set an upper limit of 0.1% for the  $\beta$ -decay branching to the 2.645 MeV level.

Brown *et al.* [4] performed a comparison of analog states in  $^{20}\text{F}$  and  $^{20}\text{Na}$  and an analysis of the available data on reactions leading to these states, and concluded that the 2.65 MeV state most likely has  $J^\pi=3^+$ . Basically, they note that the analogs of all the known states in  $^{20}\text{F}$  near this region of excitation energy can be associated with other states in  $^{20}\text{Na}$ , except for the analog of the  $3^+$  state at 2.966 in  $^{20}\text{F}$ , which then, by process of elimination, they identify with the 2.646 MeV state in  $^{20}\text{Na}$ . They argue that the  $(t,^3\text{He})$  and  $(^3\text{He},t)$  cross section angular distributions to these two analog states are consistent and that the estimated Coulomb energy shift is appropriate with this assignment.

Most recently, Page *et al.* [15] determined an upper limit of 18 meV for the resonance strength for the  $^{19}\text{Ne}(p,\gamma)^{20}\text{Na}$  reaction proceeding to this state at 2.646 MeV in  $^{20}\text{Na}$ . They performed this determination by using  $^{19}\text{Ne}$  radioactive beams and detecting the  $\beta^+$  delayed  $\alpha$  radioactivity of  $^{20}\text{Na}$ . They note that this upper limit is significantly below that estimated by Brown *et al.* and question whether the state at 2.646 MeV can, in fact, be a  $3^+$  state.

We report here new measurements of the  $^{20}\text{Ne}(p,n)^{20}\text{Na}$  reaction at 135 MeV which were performed to look for the 2.65 MeV state. These measurements are improved over the

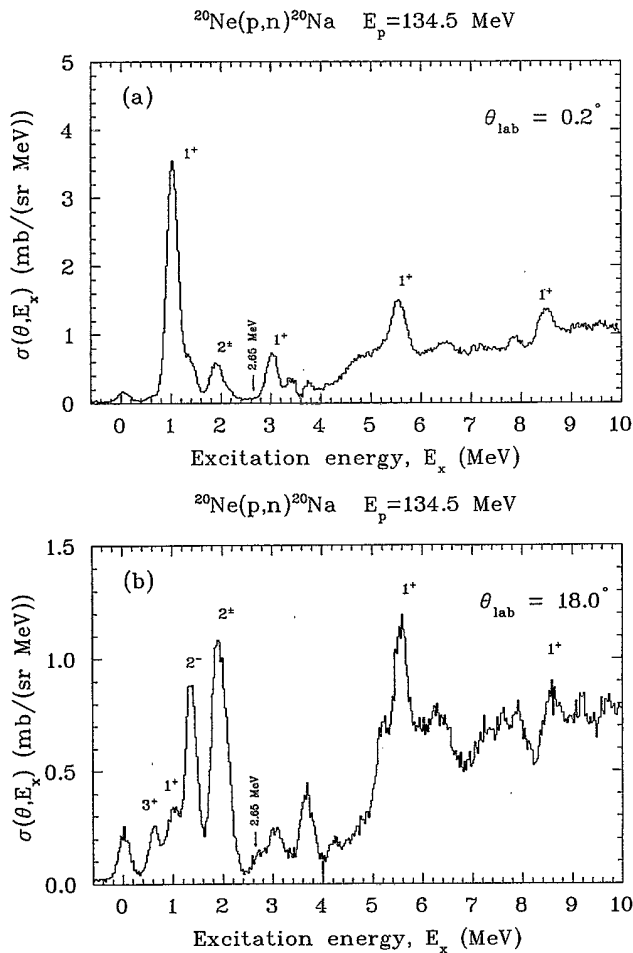


FIG. 1. Excitation-energy spectra for the  $^{20}\text{Ne}(p,n)^{20}\text{Na}$  reaction at 135 MeV at  $0.2^\circ$  and  $18^\circ$ .

earlier measurements [9] because of better counting statistics and much lower backgrounds. The improved counting statistics are from longer runs with a somewhat thicker target. The lower backgrounds were obtained by using the “stripper loop” at the IUCF to increase the time between beam bursts from  $\sim 300$  ns to  $\sim 2$   $\mu\text{s}$ , while maintaining nearly the same beam intensity. The longer time between beam bursts essentially eliminates both the “wrap-around” background from adjacent beam bursts and also the random cosmic-ray background.

With these improved measurements we were able to see a weakly excited state at 2.65 MeV. As discussed in more detail below, we see essentially no evidence for this state at  $0^\circ$ , confirming that a  $1^+$  assignment is highly unlikely. We do see this state at wider angles, with a  $\Delta l=2$  angular distribution, consistent with the proposed  $3^+$  assignment. The cross section is fitted well by a  $3^+$  distorted-wave impulse approximation (DWIA) calculation using  $1s-0d$  shell-model wave functions.

## II. EXPERIMENTAL PROCEDURE

The experiment was performed at the Indiana University Cyclotron Facility (IUCF) with the beam-swinger system. The experimental arrangement and data reduction procedures

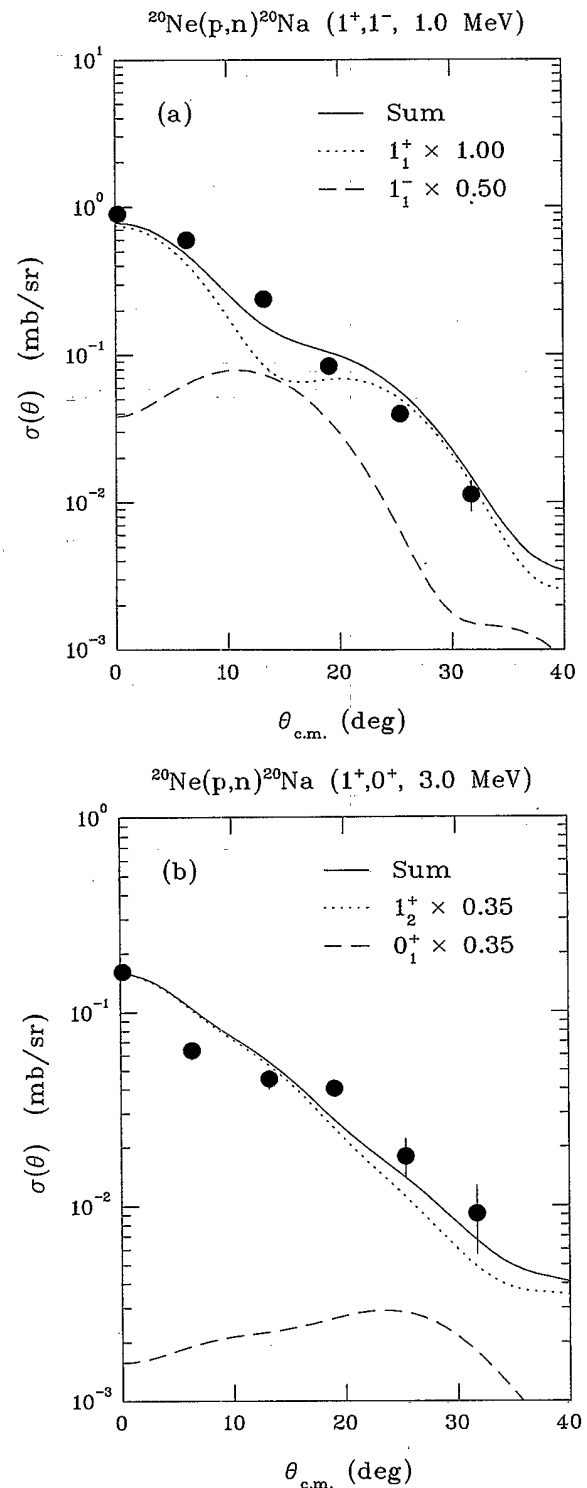


FIG. 2. Angular distributions for the  $^{20}\text{Ne}(p,n)^{20}\text{Na}$  reaction to the  $1^+$  states at 1.0 and 3.0 MeV at 135 MeV.

were similar to those described previously [9,11]. Neutron kinetic energies were measured by the time-of-flight (TOF) technique. A beam of 135 MeV protons was obtained from the cyclotron in narrow beam bursts typically 350 ps long, separated by  $\sim 2$   $\mu\text{s}$ . The long time between beam bursts was obtained by use of a small storage ring between the beam

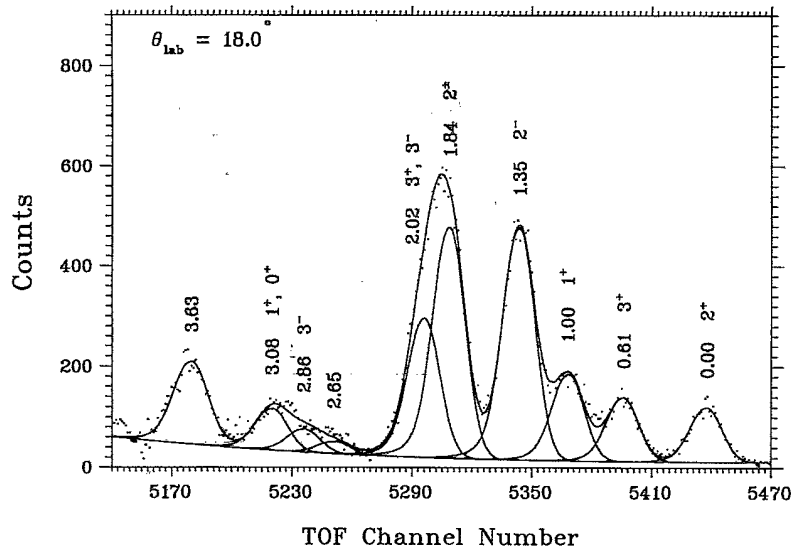


FIG. 3. The fit to the time-of-flight spectrum in the  $^{20}\text{Ne}(p,n)^{20}\text{Na}$  reaction at 135 MeV and  $18^\circ$ .

source and the main cyclotron referred to as the “stripper loop.” This long time between beam bursts eliminates “overlap” background from previous beam bursts and greatly reduces the cosmic-ray background as well. Neutrons were detected in three detector stations at  $0^\circ$ ,  $24^\circ$ , and  $45^\circ$  with respect to the undeflected proton beam. The flight paths were 125.8, 128.1, and 81.1 m ( $\pm 0.2$  m), respectively. The neutron detectors were rectangular bars of fast plastic scintillator 10.2 cm thick. Three separate detectors each 1.02 m long by 0.51 m high were combined for a total frontal area of 1.55  $\text{m}^2$  in the  $0^\circ$  and  $24^\circ$  stations. The  $45^\circ$  station had two detectors, each 1.52 m long by 0.76 m high for a total frontal area of 2.31  $\text{m}^2$ . Each neutron detector had tapered Plexiglass light pipes attached on the two ends of the scintillator bar, coupled to 12.76 cm diameter phototubes. Timing signals were derived from each end and combined in a mean-timer circuit [16] to provide the timing signal from each detector. Overall time resolutions of about 900 ps were obtained, including contributions from the beam burst width ( $\sim 350$  ps) and energy spread ( $\sim 400$  ps), energy loss in the target ( $\sim 350$  ps), neutron transit times across the 10.2 cm thickness of the detectors ( $\sim 530$  ps), and the intrinsic time dispersion of each detector ( $\sim 300$  ps). This overall time resolution provided an energy resolution of about 300 keV in the first two detector stations and about 450 keV in the widest-angle station. The large-volume detectors were described in more detail previously [17]. Protons from the target were rejected by anticoincidence detectors in front of each neutron detector array. Cosmic rays were vetoed by anticoincidence detectors on top as well as the ones at the front of each array.

The target was a low-volume cylindrical gas cell 4 cm long by 1 cm diameter. The entrance and exit windows were 25  $\mu\text{m}$  Kapton. The cell was filled to  $\sim 6$  atm absolute with  $^{20}\text{Ne}$  gas, enriched to 99.95%. Background runs were performed to subtract contributions from the Kapton windows. Time-of-flight spectra were obtained at 12 angles between  $0^\circ$  and  $63^\circ$ . Spectra from each detector were recorded at many pulse-height thresholds from 2 to 20 MeV equivalent-electron energy (MeVee). Calibration of the pulse-height response of each of the detectors was performed with a

$^{228}\text{Th}$  source ( $E_\gamma = 2.61$  MeV) and a calibrated fast amplifier. The values of the cross sections extracted for different thresholds were found to be the same within statistics.

### III. DATA REDUCTION

Excitation-energy spectra were obtained from the measured TOF spectra using the known flight paths and a calibration of the time-to-amplitude converter. The  $^{12}\text{C}(p,n)^{12}\text{N}$  reaction from carbon in the Kapton gas-cell windows was used to provide absolute reference points. At

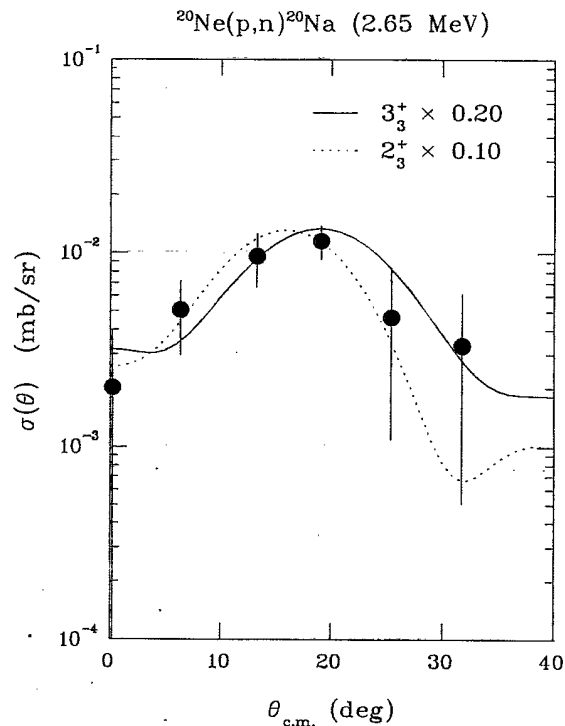


FIG. 4. Angular distribution for the  $^{20}\text{Ne}(p,n)^{20}\text{Na}$  reaction at 135 MeV to the state at 2.65 MeV. The DWIA calculations are described in the text.

forward angles, the  $^{12}\text{C}(p,n)^{12}\text{N}$  ( $1^+$ , g.s.) transition was used; at wide angles, the  $^{12}\text{C}(p,n)^{12}\text{N}$  ( $2^+$ , 0.96 MeV) transition and the  $^{12}\text{C}(p,n)^{12}\text{N}$  ( $4^-$ , 4.3 MeV) transition were employed. The  $^{20}\text{Ne}(p,n)^{20}\text{Na}$  ( $1^+$ , 1.00 MeV) transition was used at forward angles to check the accuracy of the method. This procedure is estimated to yield absolute neutron kinetic energies (and therefore excitation energies) good to  $\sim 0.05$  MeV.

In order to obtain excitation-energy spectra for the  $^{20}\text{Ne}(p,n)^{20}\text{Na}$  reaction, it was necessary to subtract the contributions from the Kapton entrance and exit windows of the gas cell. This was performed in the TOF spectra by subtracting empty-cell and/or Kapton-foil runs. The TOF spectra were aligned using the strong  $^{12}\text{C}(p,n)^{12}\text{N}$  peaks. The background run was normalized to the full-cell run by comparing the beam integrations, the target thicknesses, the computer livetimes, and the solid angles of the runs. Because there were different energy losses in the full-cell and background runs, the difference produced positive and negative swinging oscillations for subtractions of peaks, even when properly normalized. This problem was eliminated (to first order) by performing a Gaussian smearing of the background runs to broaden the TOF peaks; however, strong peaks from the carbon and oxygen in the Kapton windows still do not subtract entirely reliably. Fortunately, these peaks are present only above 3 MeV of excitation and the primary region of interest for this work is from 0 to 3 MeV of excitation.

Yields for transitions in the  $^{20}\text{Ne}(p,n)^{20}\text{Na}$  reaction were obtained by peak fitting of the TOF spectra. The spectra were fitted with an improved version of the Gaussian peak-fitting code of Bevington [18]. Examples of the peak fitting of similar ( $p,n$ ) neutron TOF spectra were presented earlier [11]. Cross sections were obtained by combining the yields with the measured geometrical parameters, the beam integration, and the target thickness. The neutron detector efficiencies were obtained from a Monte Carlo computer code [19], which was tested extensively at these energies [20,21]. The overall absolute cross sections were checked by remeasuring the known  $^{12}\text{C}(p,n)^{12}\text{N}$ (g.s.) cross section with a carbon-foil target. The uncertainty in the overall scale factor is dominated by the uncertainty in the detector efficiencies and is estimated to be  $\pm 12\%$ .

#### IV. RESULTS

Excitation-energy spectra for the  $^{20}\text{Ne}(p,n)^{20}\text{Na}$  reaction at 135 MeV are shown in Fig. 1 at  $0.2^\circ$  and  $18^\circ$ . As discussed above, these measurements were performed at the IUCF beam-swinging facility using the "stripper loop" to obtain much longer times ( $\sim 2 \mu\text{s}$ ) between beam bursts. This longer time provides backgrounds  $\sim 10\times$  smaller than in our earlier measurements. From Fig. 1, we see there is no evidence for a state at 2.65 MeV in the  $0.2^\circ$  spectrum. The cross section level is very low in this region and is essentially the same as the background level observed below the ground state. Note that  $1^+$  excitations from even-even target nuclei ( $0^+$ ) are "Gamow-Teller" ( $\Delta l=0$ ,  $\Delta s=1$ ) transitions (GT) and are known to be excited strongly in the ( $p,n$ ) reaction at this energy [10–12]. These transitions normally are peaked strongly at  $0^\circ$ . Such GT strength is seen clearly in the  $1^+$  excitations at 1.0 and 3.0 MeV in the spectrum at

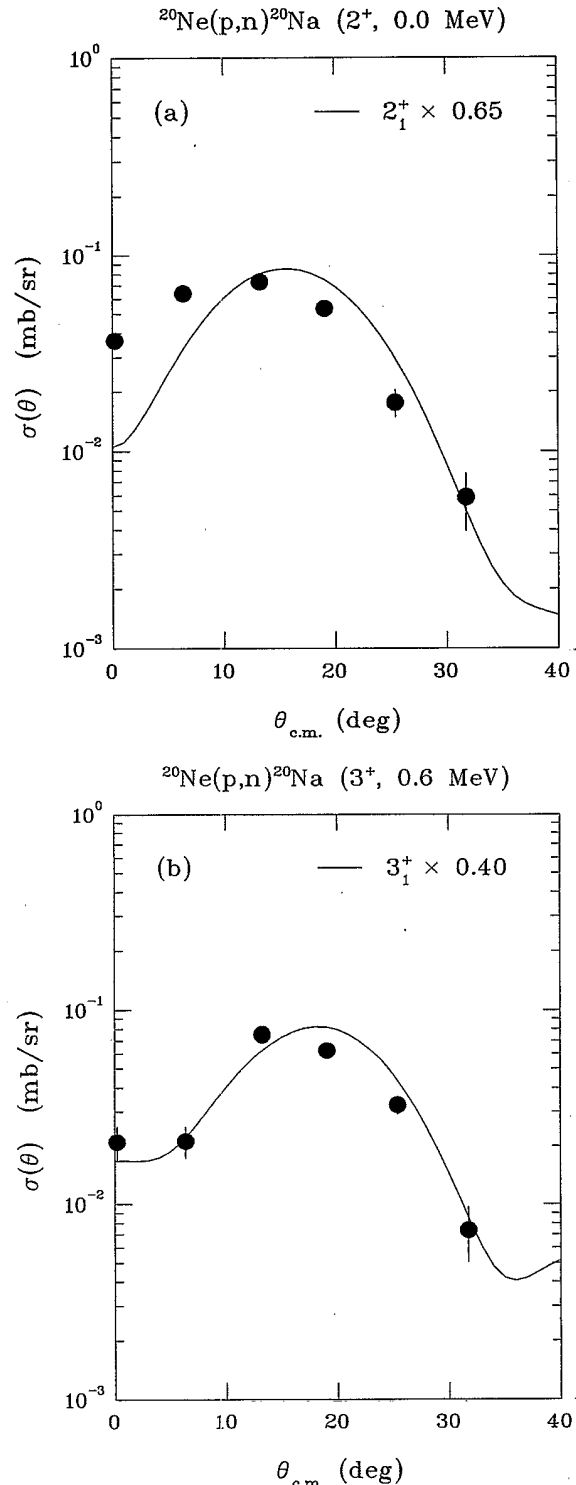


FIG. 5. Angular distributions for the  $^{20}\text{Ne}(p,n)^{20}\text{Na}$  reaction at 135 MeV to the  $2^+$  g.s. and  $3^+$  (0.6 MeV) final states. The DWIA calculations are described in the text.

$0.2^\circ$ . The angular distributions for these two transitions were extracted and are shown in Fig. 2. For comparison, we show DWIA calculations for these two levels. The DWIA calculations were performed with the code DW81 [22], using the 140 MeV, nucleon-nucleon effective interaction of Franey and

Love [23], with optical-model parameters taken from analysis of 135 MeV proton elastic scattering on  $^{16}\text{O}$  performed by Kelly *et al.* [24]. The target and final-state nuclear wave functions were calculated using the shell-model code OXBASH [25] in the  $1s-0d$  model space with the “universal”  $s-d$  interaction of Wildenthal [26]. The  $1^+$  wave functions are for the first two  $1^+$  states, predicted to be at 0.94 and 3.24 MeV, in good agreement with experiment. Shown also in Fig. 2 are DWIA calculations for the first  $1^-$  and  $0^+$  states known to be unresolved from the  $1^+$  states at 1.0 and 3.0 MeV, respectively (see Fig. 1 of Brown *et al.* [4]). As seen, the angular distributions are described well with normalization factors of 1.0 and 0.35, respectively, for the  $1^+$  transitions.

In contrast to these  $1^+$  excitations, the 2.65 MeV level shows no significant strength at  $0^\circ$ . Even if the 2.65 MeV level is an “intruder” state with predominantly multiparticle-multihole structure, one would expect some mixing with the strong  $1p-1h$   $1^+$  excitations so that one would see at least some strength at  $0^\circ$ . This result, together with results from the  $\beta$ -delayed proton-decay experiments of Kubono *et al.* [13] and Piechaczek *et al.* [14], make a  $1^+$  assignment for this state implausible.

In the  $18^\circ$  spectrum, we do see a weak excitation at 2.65 MeV. Because of the resolution of this experiment ( $\sim 300$  keV) and the weak nature of this transition, we were able to extract an angular distribution for this state only over a limited angular range. In order to extract the strength to this state, we performed careful peak fitting, requiring the fits at each angle to be consistent with the fits at neighboring angles, in terms of number and locations of peaks. The fit to the time-of-flight spectrum at  $18^\circ$  is shown in Fig. 3. All peaks in the fit correspond to known states (or complexes of states) in  $^{20}\text{Na}$ . The yield observed at 2.6 MeV is clearly above the background level observed next to it. No other state is known in this region of  $^{20}\text{Na}$ . We conclude that the strength observed here is from the 2.65 MeV level in  $^{20}\text{Na}$ .

The resulting angular distribution for the 2.65 MeV state is shown in Fig. 4. The angular distribution is peaked near  $20^\circ$ , consistent with  $\Delta l=2$ . Starting from the  $0^+$  g.s. of  $^{20}\text{Ne}$ , a single-step transition with  $\Delta l=2$ , including possible spin-flip  $\Delta s=1$ , can excite a  $1^+$ ,  $2^+$ , or a  $3^+$  final state. If the final state were  $1^+$ , it could also be excited by  $\Delta l=0$  and, as discussed above, would probably be peaked at  $0^\circ$ . In Fig. 4 we show DWIA calculations to both a  $2^+$  and a  $3^+$  final state. The final-state wave functions are for the third  $2^+$  and  $3^+$  states in the  $1s-0d$  shell-model calculations. The g.s. of  $^{20}\text{Na}$  is known to be  $2^+$ . The second  $2^+$  state is at 1.84 MeV and is believed to be the analog of a  $2^+$  state at 2.04 MeV known in  $^{20}\text{F}$ . Similarly, the first  $3^+$  state in  $^{20}\text{Na}$  is known at 0.6 MeV and the second  $3^+$  state is believed to be in the complex of states at 2.0 MeV. The angular distributions of the first  $2^+$  and  $3^+$  states are shown in Fig. 5, compared with DWIA calculations using the  $1s-0d$  wave functions for the first  $2^+$  and  $3^+$  states, respectively. As seen, these distributions are described reasonably well by the calculations. The second  $2^+$  and  $3^+$  states cannot be resolved in

the complex at 1.8–2.0 MeV in this experiment.

In Fig. 4 we see that both the  $2^+$  and  $3^+$  calculations are able to describe the angular distribution for the 2.65 MeV state. Because no analog  $2^+$  state is known near this excitation energy in  $^{20}\text{F}$ , we surmise that this level is most likely the analog of the  $3^+$  state known at 2.97 MeV in  $^{20}\text{F}$ .

## V. CONCLUSIONS

We observed the excitation of the state at 2.65 MeV in  $^{20}\text{Na}$  in the  $^{20}\text{Ne}(p,n)^{20}\text{Na}$  reaction at 135 MeV. This state is astrophysically important because it is the first state above the  $^{19}\text{Ne} + p$  threshold and will strongly affect possible breakout in the hot CNO cycle. This state was first observed in the  $^{20}\text{Ne}(^3\text{He},t)^{20}\text{Na}$  reaction at low energies and identified as a possible  $1^+$  state. We see no excitation of this state at forward angles as normally expected for such a state. Given the sensitivity of the  $(p,n)$  reaction to  $1^+$  excitations (GT strength), this  $J^\pi$  assignment seems unlikely. We see this state excited weakly at wider angles with a  $\Delta l=2$  angular distribution. The experimental cross sections are described well by a DWIA calculation to either a  $2^+$  or a  $3^+$  final state. The  $3^+$  assignment would be consistent with the  $J^\pi$  assignment of Brown *et al.*, deduced by a comparison of analog states in  $^{20}\text{F}$  and  $^{20}\text{Ne}$ . No  $2^+$  state is known in  $^{20}\text{F}$  which would be at the correct excitation energy to be the analog of the 2.65 MeV level in  $^{20}\text{Na}$ .

As discussed more fully above, one would expect that if this state were a  $1^+$  state, given the sensitivity of the  $(p,n)$  reaction to  $1^+$  excitations (GT strength), we would see this state in the  $0.2^\circ$  spectrum. Even if the state were predominantly an intruder state with multiparticle-multihole structure, one would expect at least some mixing with the strong predominantly  $1p-1h$   $1^+$  states observed at 1.0 and 3.0 MeV. We have now observed dozens of  $1^+$  excitations in various nuclei with the  $(p,n)$  reaction [9–12]. Of these, only two are observed to have angular distributions not peaked at  $0^\circ$ . These two are thought to be intruder states with predominantly multiparticle, multihole structures; but even in these two cases, some strength is observed at  $0^\circ$ . The 2.65 MeV state in  $^{20}\text{Na}$ , if it is a  $1^+$  level, would be the first example we would have of a  $1^+$  state for which we see no yield at  $0^\circ$ . Because the angular distribution is peaked at an angle consistent with  $\Delta l=2$  and is described well by a DWIA calculation for the third  $3^+$  state predicted in a  $1s-0d$  shell-model calculation, we conclude that it is more likely that this state is, in fact, the analog of the  $3^+$  level known in  $^{20}\text{F}$  at 2.966 MeV.

## ACKNOWLEDGMENTS

We would like to thank the staff of the Indiana University Cyclotron Facility for their help in mounting and running this experiment. This work was supported in part by the National Science Foundation.

- [1] M.S. Smith, P.V. Magnus, K.I. Hahn, A.J. Howard, P.D. Parker, A.E. Champagne, and Z.Q. Mao, *Nucl. Phys.* **A536**, 333 (1992).
- [2] M.A.J. Snijders, T.J. Batt, M.J. Seaton, J.C. Blades, and D.C. Morton, *Mon. Not. R. Astron. Soc.* **211**, 7 (1984).
- [3] R.E. Williams and J.S. Gallagher, *Astrophys. J.* **228**, 482 (1979).
- [4] B.A. Brown, A.E. Champagne, H.T. Fortune, and R. Sherr, *Phys. Rev. C* **48**, 1456 (1993).
- [5] L.O. Lamm, C.P. Browne, J. Görres, M. Wiescher, and A.A. Rollefson, *Z. Phys. A* **327**, 239 (1987).
- [6] S. Kubono, N. Ikeda, M. Yasue, T. Nomura, Y. Fuchi, H. Kawashima, S. Kato, H. Orihara, T. Shinozuka, H. Ohnuma, H. Miyatake, and T. Shimoda, *Z. Phys. A* **331**, 359 (1988).
- [7] L.O. Lamm, C.P. Browne, J. Görres, S.M. Graff, M. Wiescher, A.A. Rollefson, and B.A. Brown, *Nucl. Phys.* **A510**, 503 (1990).
- [8] N.M. Clarke, P.R. Hayes, M.B. Becha, C.N. Pinder, and S. Roman, *J. Phys. G* **16**, 1547 (1990).
- [9] B.D. Anderson, N. Tamimi, A.R. Baldwin, M. Elaasar, R. Madey, D.M. Manley, M. Mostajabodda'vati, J.W. Watson, W.M. Zhang, and C.C. Foster, *Phys. Rev. C* **43**, 50 (1991).
- [10] C.D. Goodman, C.A. Goulding, M.B. Greenfield, J. Rapaport, D.E. Bainum, C.C. Foster, W.G. Love, and F. Petrovich, *Phys. Rev. Lett.* **44**, 1755 (1980).
- [11] B.D. Anderson, T. Chittrakarn, A.R. Baldwin, C. Lebo, R. Madey, R.J. McCarthy, J.W. Watson, B.A. Brown, and C.C. Foster, *Phys. Rev. C* **31**, 1147 (1985).
- [12] R. Madey, B.S. Flanders, B.D. Anderson, A.R. Baldwin, C. Lebo, J.W. Watson, S.M. Austin, A. Galonsky, B.H. Wildenthal, and C.C. Foster, *Phys. Rev. C* **35**, 2011 (1987).
- [13] S. Kubono, N. Ikeda, Y. Funatsu, M.H. Tanaka, T. Nomura, H. Orihara, S. Kato, M. Ohura, T. Kubo, N. Inabe, A. Yoshida, T. Ichihara, M. Ishihara, I. Tanikata, H. Okuno, T. Nakamura, S. Shimoura, H. Toyokawa, C.C. Yun, H. Ohnuma, K. Asahi, A. Chakrabarti, T. Mukhopadhyay, and T. Kajino, *Phys. Rev. C* **46**, 361 (1992).
- [14] A. Piechaczek, M. F. Mohar, R. Anne, V. Borrel, B.A. Brown, J.M. Corre, D. Guillemaud-Mueller, R. Hue, H. Keller, S. Kubono, V. Kunze, M. Lewitowicz, P. Magnus, A.C. Mueller, T. Nakamura, M. Pfützner, E. Roeckl, K. Rykaczewski, M.G. Saint-Laurent, W.D. Schmidt-Ott, and O. Sorlin, *Nucl. Phys.* **A584**, 509 (1995).
- [15] R.D. Page *et al.*, *Phys. Rev. Lett.* **73**, 3066 (1994).
- [16] A.R. Baldwin and R. Madey, *Nucl. Instrum. Methods* **171**, 149 (1980).
- [17] R. Madey *et al.*, *Nucl. Instrum. Methods* **214**, 401 (1983).
- [18] P.R. Bevington, *Data Reduction and Error Analysis for the Physical Sciences* (McGraw-Hill, New York, 1969), p. 237.
- [19] R. Cecil, B.D. Anderson, and R. Madey, *Nucl. Instrum. Methods* **161**, 439 (1979).
- [20] J.W. Watson, B.D. Anderson, A.R. Baldwin, C. Lebo, B. Flanders, W. Pairsuwan, R. Madey, and C.C. Foster, *Nucl. Instrum. Methods* **215**, 413 (1983).
- [21] J. D'Auria, M. Dombisky, L. Moritz, T. Ruth, G. Sheffer, T.E. Ward, C.C. Foster, J.W. Watson, B.D. Anderson, and J. Rapaport, *Phys. Rev. C* **30**, 1994 (1984).
- [22] Program DWBA70, R. Schaeffer and J. Raynal (unpublished); extended version DW81 by J.R. Comfort (unpublished).
- [23] M.A. Franey and W.G. Love, *Phys. Rev. C* **31**, 488 (1985).
- [24] J. Kelly, Ph.D. dissertation, Massachusetts Institute of Technology, 1981.
- [25] Computer code OXBASH, B.A. Brown, A. Etchegoyen, W.D.M. Rae, and N.S. Goodwin (unpublished).
- [26] B.H. Wildenthal, *Prog. Nucl. Phys.* **11**, 5 (1984).